Lung and Kidney Perfusion Deficits Diagnosed by Dual-Energy Computed Tomography in COVID–19 Patients: Evidence Supporting Systemic Microangiopathy

Ilkay S. Idilman
Hacettepe University, Faculty of Medicine https://orcid.org/0000-0002-1913-2404
Gulcin Telli Dizman
Hacettepe University, Faculty of Medicine
Selin Ardali Duzgun
Hacettepe University, Faculty of Medicine
Ilim Irmak
Hacettepe University, Faculty of Medicine
Musturay Karcaaltincaba
Hacettepe University, School of Medicine
Ahmet Cagkan Inkaya
Hacettepe University, Faculty of Medicine
Figen Basaran Demirkazik
Hacettepe University, Faculty of Medicine
Gamze Durhan
Hacettepe University, Faculty of Medicine
Meltem Gulsun Akpinar
Hacettepe University, Faculty of Medicine
Orhan Macit Ariyurek
Hacettepe University, Faculty of Medicine
Erhan Akpinar
Hacettepe University, Faculty of Medicine
Jordi Rello
University Hospital Vall d'Hebron, Department of General Area Intensive Medicine
Murat Akova
Hacettepe University, Faculty of Medicine
Deniz Akata (akataden@gmail.com)
Hacettepe University, Faculty of Medicine

Research Article

Keywords: COVID-19, Computed tomography angiography, Lung, Kidney, Perfusion

Posted Date: May 29th, 2020

DOI: https://doi.org/10.21203/rs.3.rs-32474/v1

Version of Record: A version of this preprint was published on August 29th, 2020. See the published version at https://doi.org/10.1007/s00330-020-07155-3.

Abstract

Objectives: There is increasing evidence of thrombotic events occurring in patients with coronavirus disease (COVID-19). We evaluated dual-energy computed tomography (DECT) findings, particularly lung and kidney perfusion, in non-intubated COVID-19 patients.

Methods: Thirty-one COVID-19 patients who underwent pulmonary DECT angiography between March 15 and April 30, 2020, and were suspected of having pulmonary thromboembolism were included. Pulmonary and kidney images were reviewed. Qualitative and quantitative analyses of the perfused blood volume and iodine maps were performed.

Results: DECT images showed perfusion deficits (PDs) in eight patients (25.8%), which were not overlapping with areas of ground-glass opacity or consolidation. Two patients had pulmonary thromboembolism confirmed by CT angiography. Five of 10 patients who had been infected for more than 5 days had PDs documented. Patients with PDs had a longer hospital stay (12.25 ± 8.81 vs 6.83 ± 5.04 days, p= 0.14), higher intensive care unit admission rates (37.5% vs 4.3%, p=0.02), higher CT scores (13.3 ± 8.2 vs 5 ± 5.4, p= 0.02) and more severe disease (50% vs 4.3%, p=0.01). In the PD group, serum ferritin, aspartate aminotransferase (AST), fibrinogen, D-dimer, C-reactive protein (CRP), and troponin levels were significantly higher, whereas albumin level was lower ($p<0.05$). D-dimer levels $\geq$ 0.485 ug/L predicted PD with 100% specificity and 87% sensitivity (AUROC: 0.957). Renal iodine maps showed heterogeneous enhancement consistent with perfusion abnormality in 13 patients (50%). Sodium levels were significantly lower in this group (p=0.03).

Conclusions: Pulmonary perfusion abnormalities in COVID 19 patients is associated with more severe disease and in most of the patients can occur without macroscopic pulmonary thromboembolism. High rate of kidney perfusion abnormalities suggests subclinical systemic microvascular obstruction.

Key Points

-Pulmonary DECT detects pulmonary perfusion abnormalities in COVID–19 patients which is associated with more severe disease.

-A cut-off value of 0.485 ug/L for D-dimer plasma levels predicted lung perfusion deficits with 100% specificity and 87% sensitivity (AUROC: 0.957).

-Perfusion abnormalities in the kidney reflects a subclinic systemic microvascular obstruction in these patients.

Introduction

Radiological imaging of the lungs has become a diagnostic tool for coronavirus disease (COVID–19), due to the low sensitivity of real-time, reverse-transcription polymerase chain reaction (RT-PCR) tests from

swab samples [1–3]. Several imaging characteristics have been described including single or multiple focal ground-glass opacities (GGOs) in the lungs [4, 5]. Recently, multi-organ endotheliitis was identified in patients with COVID–19 which may be due to the widespread distribution and co-expression of ACE–2 and S-protein-specific proteases [6–8]. Microangiopathic lesions with thrombosis have been shown in pathological specimens from the lungs of critically ill patients with COVID–19 [9], and anticoagulant therapy has been shown to improve their prognosis [10].

Dual-energy computed tomography (DECT) allows quantification of iodine uptake, which is a good surrogate for pulmonary parenchymal perfusion [11–12]. This technique can be used for CT angiography and allows for the evaluation of perfusion and the presence of pulmonary artery thrombus simultaneously, without increasing radiation dose as compared to standard CT. Iodine maps obtained with this method can also demonstrate perfusion of kidneys, which are included at the caudal aspect of DECT angiography. Here, we aimed to evaluate DECT findings in patients with COVID–19, particularly pulmonary parenchymal and kidney perfusion abnormalities.

Materials And Methods

Patients and clinical follow-up

Thirty-one adults (>18 years) diagnosed with COVID–19 and hospitalized between March 15, 2020 and April 30, 2020 in Hacettepe University Adult Hospital, Ankara, Turkey (a 1000-bed tertiary care facility), who underwent DECT angiography because of suspected pulmonary thromboembolism (PE) were analyzed. COVID–19 was diagnosed using reverse-transcription polymerase chain reaction (RT-PCR) on nasopharyngeal smears. According to national guidelines, all RT-PCR confirmed COVID–19 patients were considered for hospital admission. Electronic records of the Hacettepe University Hospital and follow-up charts of the patients were reviewed by the authors (ISI, GTD, ACI) and saved in an electronic database. Gender, age, comorbidities, fever, $SaPO_2$, daily follow-up records, medications to treat comorbidities and COVID–19 and results of blood biochemistry, complete blood count, coagulation tests, C-reactive protein (CRP), procalcitonin, urinalysis were also recorded in an electronic case record form. Confirmed patients that were evaluated as needing treatment as per the national guidelines were admitted to isolation wards. A suspected PE was based on clinical findings and/or elevated D-dimer serum levels (>1000 ng/mL). Patients were informed about the radiological procedure and provided informed consent. Pregnant women and those declining consent were excluded. Clinical disease severity for COVID–19 was defined as proposed by Feng et al [13]. In brief, patients are categorized into four types. Type one had mild symptoms and no abnormal radiological findings. Type two had moderate symptoms and evidence of pneumonia on chest CT. Type three patients had either a high respiratory rate (≥30/min) or SaO_2 (≤93%) or low oxygen partial pressure/inspired oxygen fraction (≤300 mmHg) in arterial blood. Type four patients needed mechanical ventilation or had shock or organ dysfunction needing intensive care unit (ICU) admission.

CT acquisition protocol and DECT Post-processing and Image Reconstruction

The DECT angiography images were obtained by third-generation dual-source CT (Somatom Force, Siemens Healthineers, Erlangen). Patients received intravenously 50–60mL iohexol (Omnipaque 350; GE Healthcare, Princeton, NJ), at a rate of 4.0 mL/sec via antecubital intravenous catheter, followed by a 40-ml saline chaser bolus. A region of interest (ROI) was placed over the pulmonary artery and acquisition was started when the ROI reaches 100 HU with a delay of 5 s. Craniocaudal acquisition was set with the following parameters: 80/140Sn kVp, modulated mA (CareDose 4D, Siemens Healthineers, Erlangen, Germany) with reference 80 mAs, rotation time 0.25 s, with a pitch of 0.7 and a collimation of (64 x 0.6 mm x 2).

Perfused Blood Volume (PBV) images and iodine maps were generated using DECT post-processing softwares (“Lung PBV” and “Virtual unenhanced” in syngo Dual Energy; Siemens Healthineers) on a dedicated workstation.

The DECT scanner generates three different series of images: 80-kV images, 140-kV images, and weighted-average images (similar to 120-kVp scan of the abdomen). Images were loaded to a dedicated DE post-processing workstation (Syngo Via VB10; Siemens Medical Solutions). By using Lung PBV application, iodine uptake distribution can be mapped to visualize perfusion. This calculation is based on a so-called three-material decomposition: Assuming that every voxel in the lung is composed of air, soft tissue, and iodine, the algorithm generates a map that encodes the iodine distribution in each individual CT voxel. To generate lung perfusion maps, we put an ROI on the pulmonary artery. We used scale factor of 0.15 to normalize the perfusion of the lung parenchyma. Lung volume and subvolume, mean contrast (iodine) enhancement in HU and relative enhancement in percentage can be measured automatically. In addition to lung PBV images, virtual noncontrast (VNC) image and iodine maps were obtained by using “virtual unenhanced” software. Iodine map can be superimposed on weighted-average or VNC images for visualization of iodine uptake distribution and anatomic information at the same time.

Morphologic images, lung perfusion maps and iodine maps were analyzed by three experienced readers (with 14, 24 and 32 years of CT experience). Image quality on the perfusion map was recorded as either excellent (no artifacts), good (minor artifacts), moderate (still able to assess iodine distribution), or poor (impossible to assess iodine distribution). The pulmonary DECT angiography image quality was excellent in 2 cases, good in 21 cases and moderate in 8 patients. The perfusion map images were then reviewed for the presence of any deficit. Perfusion map deficits were characterized as either overlapping with GGO or consolidation, not overlapping with GGO or consolidation, or band-like deficits consistent with artifact, often due to cardiac motion or beam hardening from contrast material within the superior vena cava or innominate vein. The lesions on CT images that are over 1 cm were also evaluated and recorded as GGO or consolidation and iodine uptake of these lesions was measured with three elliptic round of interest (ROI) on iodine map images and mean value was calculated.

Lung CT images were classified according to the extent of GGOs and the presence of consolidation and crazy-paving pattern in the lobes. The scores were defined as follows: 0 (none), one (affecting less than 5% of the lobe), two (affecting 5–25% of the lobe), three (affecting 26–49% of the lobe), four (affecting 50–75% of the lobe) and five (affecting more than 75% of the lobe) [14]. If the crazy-paving pattern or consolidation appeared in one lobe, the CT score was increased by one for each of them. Therefore, a maximum CT score of seven was possible for each lobe. The total CT score was calculated by summing the five lobe scores (range from 0 to 35). Perfusion images were graded according to the extent of perfusion deficits (PDs). The grades were defined as follows: 0 (no PD), one (affecting only one area), two (affecting 1–3 PD areas), three (multiple bilateral PDs >4–10 areas), and four (bilateral PDs disseminated in all segments covering >50% of the total lung perfusion areas).

In 5 patients, pulmonary CTA examination did not include more than 75% of the longitudinal diameter of the kidneys and excluded from the kidney analyses. The kidneys were analyzed on VNC, iodine map and mixed DECT images. An ROI was placed over the abdominal aorta to normalize contrast enhancement before the analysis. Visual analysis of these images were performed by three radiologists in consensus. Homogeneous pattern on iodine map is defined as smooth appearance without low iodine uptake areas; heterogeneous pattern is defined as mottled appearance with alternating low and high iodine uptake. Density measurements were made on cortex of the kidney on iodine map and VNC images. A freehand ROI was placed on the cortex of the kidney and density measurements were recorded. Also, mottled areas were also evaluated by a using a circular region-of-interest of approximately 5 mm^2.

Ethics

Hacettepe University Ethics Board for Non-Interventional Studies reviewed and approved the study protocol (Decision no: 17.04.2020 - GO 20/388).

Statistical analysis

Categorical data are presented as numbers (percentages), and continuous variables are expressed as means ± standard deviations unless otherwise stated. Categorical data were compared using the Pearson Chi-square test/Fisher's exact test, and continuous variables were compared using the Student's t-test or Mann-Whitney U-test according to the distribution of data. The degree of association between continuous and/or ordinal variables was calculated using Pearson's correlation coefficient or Spearman's rho analysis according to the distribution of data. A one-way analysis of variance (ANOVA) or Kruskal–Wallis analysis was performed for comparing continuous variables in different PD grades. A two-tailed p-value of <0.05 was considered statistically significant. A receiver operating characteristic (ROC) curve analysis was performed to define the value of laboratory parameters in predicting PD.

Results

A total of 31 patients (M/F 16/15) with COVID–19, who underwent pulmonary DECT angiography for a suspected PE were retrospectively analyzed. The mean age of the participants was 39.2 ± 12 years (range 23–65 years) (Table 1). Disease severity upon presentation was mild, with 19.3% of patients requiring oxygen therapy. Two patients had hypertension, two had asthma, two had arrhythmia, two had coronary heart disease, one had diabetes, one had hypothyroidism, one had Crohn's disease, and one had insulinoma. None of the patients received therapeutic and prophylactic anticoagulation before CT imaging. All CT scans were performed on non-intubated subjects, and there was a median of three days from symptom onset to the CT scan (interquartile range (IQR): two to 11). In the analysis of lung CT images, seven patients had no lung lesions, and the mean CT score was 7.6 ± 7.1 (0–22). There were significantly positive correlations between the CT score and age ($p = 0.01$, $r = 0.468$) and severity of the disease ($p<0.001$, $r = 0.760$). Similarly, correlations were found between the CT score and various laboratory values (Suppl. Table 1).

DECT angiography identified overt PE in only two patients (6.5%). In lung perfusion maps, these patients had PDs corresponding to the areas with vascular occlusion and areas of decreased perfusion without visible thrombus (Fig. 1). Apart from these two cases, PDs were visualized in six more patients who had no detectable emboli in the pulmonary arteries (Fig. 2). Patients with PDs were symptomatic for a median (IQR) overall time of 11.5 (4–18) days. The PDs did not overlap with GGOs or consolidation. In the subgroup analysis, patients with PDs had a prolonged hospital stay (12.28 ± 8.81 vs. 6.83 ± 5.04 days, $p = 0.14$), higher rate of ICU admission (37.5% vs. 4.3%, $p = 0.04$), higher CT score (13.3 ± 8.2 vs. 5 ± 5.4, $p = 0.06$) and more severe disease (50% versus 4.3%, $p = 0.01$). The only significantly more frequent clinical symptom in patients with PDs was a sore throat (50% versus 13%, $p = 0.03$). Ferritin, AST, fibrinogen, D-dimer, CRP, and troponin plasma levels were significantly higher, and albumin levels were significantly lower in patients with PDs (Table 2). A receiver operator characteristic (ROC) curve analysis revealed that D-dimer plasma levels ≥ 0.485 ug/L predicted lung PD with 100% specificity and 87% sensitivity (area under the (AU)ROC: 0.957) with a positive predictive value of 80% and a negative predictive value of 100%.

When we grouped patients according to the extent of PDs, there were statistically significant differences in terms of clinical classification, CT score, presenting symptoms like sore throat and need for oxygen therapy (Table 3). When comparing 1–2 grade PD patients and 3–4 grade PD patients, the median duration after infection onset was four vs. 14 days ($p = 0.26$). D-dimer was the only laboratory variable related to PD ($p = 0.01$).

In the quantitative analysis of the perfusion maps, there were lower relative enhancement values in the patients with PDs in comparison with patients without PDs, with no statistical significance (66% ± 34.8% versus 73.1% ± 27.5%, $p = 0.56$) (Suppl. Table 2). Among 80 lung lesions, 38 lesions were GGOs, and the remaining 42 lesions were areas of consolidation. The virtual non-contrast (VNC) density and iodine uptake of these lesions were –820.2 HU ± 40.9 HU and 22.3 HU ± 12.4 HU, respectively. There was significantly increased iodine uptake in consolidations compared with GGOs (45.1±21.2 HU vs. 29.3±13.9 HU, $p = 0.002$, Fig. 3).

A total of 51 kidneys were evaluated in 26 patients (one patient had a single kidney). In five patients, kidney images were non-diagnostic, and they were excluded from the analysis. In 13 patients (50 %), there was a diffuse heterogeneous enhancement in the cortex of both kidneys. Focal heterogeneous enhancement in the left upper pole of the kidney was detected in two patients. The typical findings were sub-centimeter moth-eaten like low iodine uptake areas in the cortex of the kidneys. None of the patients had evidence of abnormal kidney function. Serum sodium levels were lower ($p = 0.03$) in these patients as compared with those who had normal kidney perfusions (Suppl. Table 3). The overall iodine uptake of the kidney, which reflects perfusion of the kidney was lower in patients with a heterogeneous pattern in comparison with normal ones (78 HU ± 26.2 HU versus 136.5 HU ± 39.5 HU $p<0.001$ for the right kidney and 76.9 HU ± 30.7 HU versus 132.8 ± 43.9 HU $p = 0.001$ for the left kidney) (Suppl. Table 4). Quantitative measurements revealed statistically significant lower perfusion in mottled areas in patients with a heterogeneous pattern (25.4 HU ± 12.6 HU versus 110.7 HU ± 31 HU, respectively $p<0.001$). Contrastingly, these low perfused areas had statistically significant higher VNC values compared to the normal parenchyma (52 HU ± 19 HU versus 14.3 HU ± 9.3 HU, $p<0.001$).

All patients survived through the study period and were discharged from the hospital. We repeated DECT imaging in two patients within one month. Previous PDs were improved in the first patient (Fig. 4). PDs in the second patient who had a pulmonary thromboembolism were improved with stable findings related to the emboli.

Discussion

Among 31 non-intubated patients with mild COVID–19, DECT angiography demonstrated PDs in the lungs of 60% of patients five or more days after symptom onset and in half of the kidneys assessed. Only two of them had major lung vascular occlusion leading to PE, and none had major renal dysfunction. In the quantitative analysis, we observed lower relative enhancement values in patients with PDs in comparison with patients having no PDs, confirming decreased perfusion in this patient group. Although clinical signs did not anticipate the presence of perfusion abnormalities, they were significantly associated with some biomarkers such as higher D-dimer plasma concentrations, CRP, ferritin, or troponin. Increased D-dimer levels were demonstrated to be an early clinical predictor of perfusion abnormalities, with a threshold of 0.485 ug/L predicting PD with 100% specificity and 87% sensitivity. In the analysis of 80 lung lesions observed in these patients, we observed a lower iodine uptake in the GGOs compared with consolidations, which is consistent with increased perfusion in the lesions in the later phase of the disease. In addition, we observed heterogeneous enhancement consistent with perfusion abnormalities in the kidneys of 50% of the study population.

A recent study reported that 23% of patients with COVID–19 who had severe clinical features suffered from a PE. These scholars suggested the use of contrast-enhanced CT rather than routine non-contrast CT in these patients [15]. We observed overt PE in only two patients (6.5%) with mild clinical symptoms. However, we demonstrated PDs in 25.8% of our patient population with worse clinical and laboratory parameters.

Iodine maps and perfusion blood volume (PBV) images generated by DECT provide information about perfusion of the lungs by assessing iodine distribution in the lungs. In PE, PBV images demonstrate acute infarction as a peripheral wedge-shaped area of non-enhancement that is usually bigger than the pulmonary opacity seen on conventional CT images [16]. In patients with pneumonia and atelectasis, the abnormalities seen on conventional CT images and PBV are similar in size with heterogeneously decreased or increased iodine distribution in the former and increased iodine distribution in the latter [17].

In our study population, we demonstrated PDs in lungs that do not overlap with GGOs or consolidation and are also not associated with major vessel occlusion. A similar observation was recently described [18]. Angiopathic microvascular occlusion has been proposed as the underlying mechanism [19].Another recent study showed fibrin thrombi of small arterial vessels less than 1 mm in diameter in 33 of 38 patients with high D-dimer levels [20]. Increased D-dimer levels in our patients with PDs are supportive of these observations. DECT can improve the detection of small pulmonary emboli that may otherwise be missed with conventional CT angiography [21]. In our population, we observed lower iodine uptake in GGOs compared with consolidations. This finding can be explained by the predominant effect of edema in the early phase of the disease and increased perfusion in the later phases.

Viral infections can trigger systemic inflammation and activate a coagulation cascade through different mechanisms [22]. Inflammatory cytokines, complement activation, endothelial infection, and endotheliitis are the leading causes of thrombosis in patients with COVID–19 [8, 23]. Furthermore, platelet activation through Fc receptor binding may also initiate a coagulation cascade [24]. Therefore, thromboprophylaxis with low molecular weight heparin (LMWH) has been proposed in these patients unless contraindications are present [25]. In this study, none of the patients received thromboprophylaxis before CT imaging. Subsequently, patients with a confirmed PE received anticoagulant treatment, and the remaining patients received thromboprophylaxis with LMWH. Early commencement of thromboprophylaxis might have also contributed to the favorable survival rate of our patients. In addition, hydroxychloroquine treatment used in most of the patients might have prevented progression of PDs to major thromboembolic events as this drug has been previously shown to prevent thrombosis in patients with systemic lupus erythematosus and antiphospholipid antibodies [26].

We also showed heterogeneous kidney enhancement in DECT analysis in 13 of 26 (50%) patients, which is suggestive of microvascular occlusion. The patients had no detectable major kidney dysfunction, but lower serum sodium levels compared to the patients with normal kidneys. ACE2, the functional receptor of severe acute respiratory syndrome coronavirus 2 (SARS-CoV–2) and its S protein priming proteases have been found to be widespread in the vascular endothelium and several organ systems [8]. Together with the findings of a recent study that showed the presence of viral elements within endothelial cells, a COVID–19 endotheliitis could explain the systemic impaired microcirculatory function in different vascular beds. In support of this proposition, another recent study observed tissue damage consistent with complement-mediated microvascular injury in the lungs and/or skin of five individuals with severe COVID–19 using pulmonary and cutaneous biopsy and autopsy samples [23]. Another study showed direct parenchymal infection of tubular epithelial cells and podocytes with marked erythrocyte

aggregation in patients with severe COVID–19 [27]. The observed high VNC values of the hypo-perfused areas may explain such aggregates or thrombosis in our study population. None of our patients developed kidney dysfunction which may be explained with the relatively small percentage of kidney involvement and the early LMWH treatment.

There are several limitations to this study. We did not perform a dedicated CT perfusion study on the lungs and kidneys. However, DECT is a widely used quantitative technique and enables measurement of iodine uptake as reliable indirect evidence of perfusion. Secondly, our sample size was small which can be explained by pulmonary CTA with DECT is not a routine CT protocol in patients with COVID–19 and retrospective nature of the study. Third limitation is our sample contained patients with mild COVID–19 that did not require intubation and/or mechanical ventilation. The patients in this cohort were relatively young with few comorbidities, and findings may differ under other conditions. On the other hand, this cohort strengthens the thesis of COVID–19 induced perfusion abnormalities. A selection bias cannot be completely ruled out. Similarly, the data cannot be generalized because cohorts with different symptoms or duration of illness can present other abnormalities.

Conclusion

In conclusion, we found that a large proportion of patients with mild to moderate COVID–19 had PDs in their lungs and kidneys, which may indicate the presence of systemic microangiopathy with micro-thrombosis. These findings help to understand the physiology of hypoxemia and may have implications regarding the management of patients with COVID–19, such as early indications for thromboprophylaxis or anticoagulation and optimizing strategies for oxygenation.

Abbreviations

CT: Computed tomography

COVID–19: Coronavirus 2019 disease

DECT: Dual-energy computed tomography

GGO: Ground glass opacity

HU: Hounsfield Unit

ICU: Intensive Care Unit

PD: Perfusion deficit

PE: Pulmonary embolism

VNC: Virtual noncontrast

Declarations

Funding information: The authors state that this work has not received any funding.

Compliance with ethical standards

Guarantor: The scientific guarantor of this publication is Deniz Akata, M.D.

Conflict of interest: The authors of this manuscript declare no relationships with any companies whose products or services may be related to the subject matter of the article.

Statistics and biometry: No complex statistical methods were necessary for this paper.

Informed consent: Written informed consent was not required for this study due to the retrospective design

Ethical approval: Hacettepe University Ethics Board for Non-Interventional Studies reviewed and approved the study protocol (Decision no: 17.04.2020 - GO 20/388).

Methodology • Retrospective • Observational • Performed at one institution

References

1. Ai T, Yang Z, Hou H, et al (2020) Correlation of Chest CT and RT-PCR Testing in Coronavirus Disease 2019 (COVID-19) in China: A Report of 1014 Cases. Radiology. DOI: 10.1148/radiol.2020200642
2. Fang Y, Zhang H, Xie J, et al (2020) Sensitivity of chest CT for COVID-19: Comparison to RT-PCR. Radiology. DOI: 10.1148/radiol.2020200432
3. Xie X, Zhong Z, Zhao W, Zheng C, Wang F, Liu J (2020) Chest CT for Typical 2019-nCoV Pneumonia: Relationship to Negative RT-PCR Testing. Radiology. DOI: 10.1148/radiol.2020200343
4. Jin YH, Cai L, Cheng ZS, et al (2020) A rapid advice guideline for the diagnosis and treatment of 2019 novel coronavirus (2019-nCoV) infected pneumonia (standard version). Mil Med Res. 7:4
5. Salehi S, Abedi A, Balakrishnan S, Gholamrezanezhad A (2020) Coronavirus disease 2019 (COVID-19): a systematic review of imaging findings in 919 patients. *AJR Am J Roentgenol*. DOI:10.2214/AJR.20.23034
6. Letko M, Marzi A, Munster V (2020) Functional assessment of cell entry and receptor usage for SARS-CoV-2 and other lineage B betacoronaviruses. Nat Microbiol. 5:562-569.
7. Sungnak W, Huang N, Bécavin C, et al (2020) SARS-CoV-2 entry factors are highly expressed in nasal epithelial cells together with innate immune genes. Nat Med. DOI: 10.1038/s41591-020-0868-6
8. Varga Z, Flammer AJ, Steiger P, et al (2020) Endothelial cell infection and endotheliitis in COVID-19. 395:1417–1418.

9. Luo W, Yu H, Gou J et al (2020) Clinical Pathology of Critical Patient with Novel Coronavirus Pneumonia (COVID-19). Preprints. 2020020407.
10. Tang N, Bai H, Chen X, Gong J, Li D, Sun Z (2020) Anticoagulant treatment is associated with decreased mortality in severe coronavirus disease 2019 patients with coagulopathy. J Thromb Haemost. 18:1094-1099.
11. Fuld MK, Halaweish AF, Haynes SE, Divekar AA, Guo J, Hoffman EA (2013) Pulmonary perfused blood volume with dual-energy CT as surrogate for pulmonary perfusion assessed with dynamic multidetector CT. Radiology. 267:747-56.
12. Aran S, Daftari Besheli L, Karcaaltincaba M, Gupta R, Flores EJ, Abujudeh HH (2014) Applications of dual-energy CT in emergency radiology. AJR Am J Roentgenol 202:314-24.
13. Feng Y, Ling Y, Bai T, et al (2020) COVID-19 with Different Severity: A Multi-center Study of Clinical Features. Am J Respir Crit Care Med. DOI: 10.1164/rccm.202002-0445OC
14. Huang G, Gong T, Wang G, et al (2020) Timely Diagnosis and Treatment Shortens the Time to Resolution of Coronavirus Disease (COVID-19) Pneumonia and Lowers the Highest and Last CT Scores From Sequential Chest CT. AJR Am J Roentgenol. 30:1-7.
15. Grillet F, Behr J, Calame P, Aubry S, Delabrousse E (2020) Acute Pulmonary Embolism Associated with COVID-19 Pneumonia Detected by Pulmonary CT Angiography. Radiology. DOI: 10.1148/radiol.2020201544
16. Lang M, Som A, Mendoza DP, et al (2020) Hypoxaemia related to COVID-19: vascular and perfusion abnormalities on dual-energy CT. Lancet Infect Dis. DOI: 10.1016/S1473-3099(20)30367-4
17. Otrakji A, Digumarthy SR, Lo Gullo R, Flores EJ, Shepard JA, Kalra MK (2016) Dual-Energy CT: Spectrum of Thoracic Abnormalities. Radiographics. 36:38-52.
18. Lang M, Som A, Mendoza DP, et al (2020) Hypoxaemia related to COVID-19: vascular and perfusion abnormalities on dual-energy CT. Lancet Infect Dis. DOI:10.1016/S1473-3099(20)30367-4
19. Oudkerk M, Büller HR, Kuijpers D, et al (2020) Diagnosis, Prevention, and Treatment of Thromboembolic Complications in COVID-19: Report of the National Institute for Public Health of the Netherlands. Radiology. DOI: 10.1148/radiol.2020201629
20. Carsana L, Sonzogni A, Nasr A, et al (2020) Pulmonary post-mortem findings in a large series of COVID-19 cases from northern Italy. medRxiv. DOI:10.1101/2020.04.19.20054262
21. Weidman EK, Plodkowski AJ, Halpenny DF, et al (2018) Dual-energy CT angiography for detection of pulmonary emboli: incremental benefit of iodine maps. Radiology. 289:546–553
22. Subramaniam S, Scharrer I (2018) Procoagulant activity during viral infections. Front Biosci Landmark Ed. 23:1060–1081
23. Magro C, Mulvey JJ, Berlin D, et al (2020) Complement associated microvascular injury and thrombosis in the pathogenesis of severe COVID-19 infection: a report of five cases. Transl Res. DOI:10.1016/j.trsl.2020.04.007

24. Zhang Y, Xiao M, Zhang S, et al (2020) Coagulopathy and antiphospholipid antibodies in patients with Covid-19. N Engl J Med. 382:38
25. Thachil J, Tang N, Gando S, et al (2020) ISTH interim guidance on recognition and management of coagulopathy in COVID-19. J Thromb Haemost. 18:1023–1026
26. Petri M (2011) Use of hydroxychloroquine to prevent thrombosis in systemic lupus erythematosus and in antiphospholipid antibody-positive patients. Curr Rheumatol Rep. 13:77–80
27. Su H, Yang M, Wan C, et al (2020) Renal histopathological analysis of 26 postmortem findings of patients with COVID-19 in china. Kidney International. DOI:10.1016/j.kint.2020.04.003

Figures

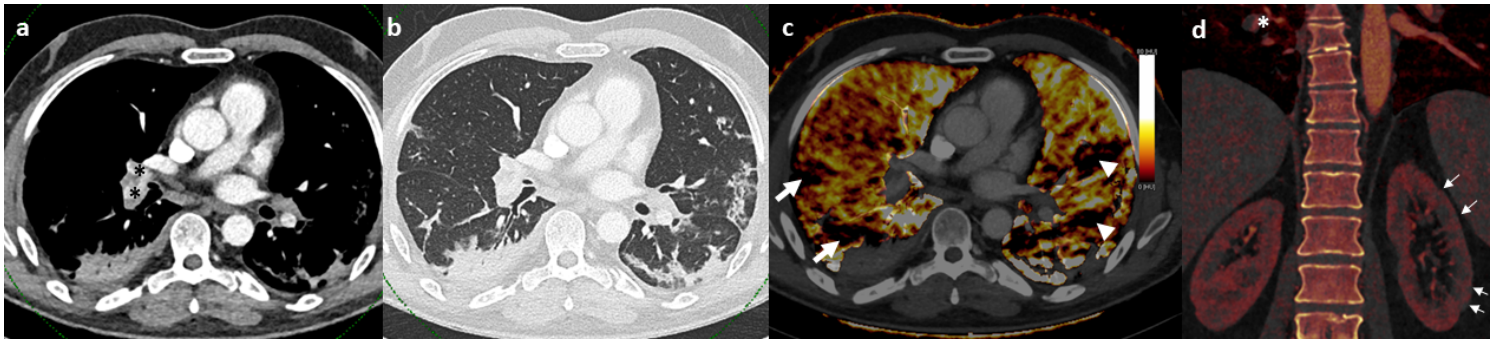

Figure 1

A 47-year-old male with coronavirus disease 2019 (COVID 19). Pulmonary thromboembolism (PE) can be seen in the right lobar and segmental pulmonary arteries (*) on pulmonary dual-energy computed tomography (DECT) angiography images (a and b). On the perfusion map images (c), perfusion deficits due to the PE (arrows) can be seen in the right lung. There are also perfusion deficits in the left lobe, which are not associated with vessel occlusion or parenchymal findings (arrowheads). On coronal renal perfusion images (d), heterogeneous kidney enhancement (arrows), and a PE in the right lower lobe pulmonary artery (*) can be seen.

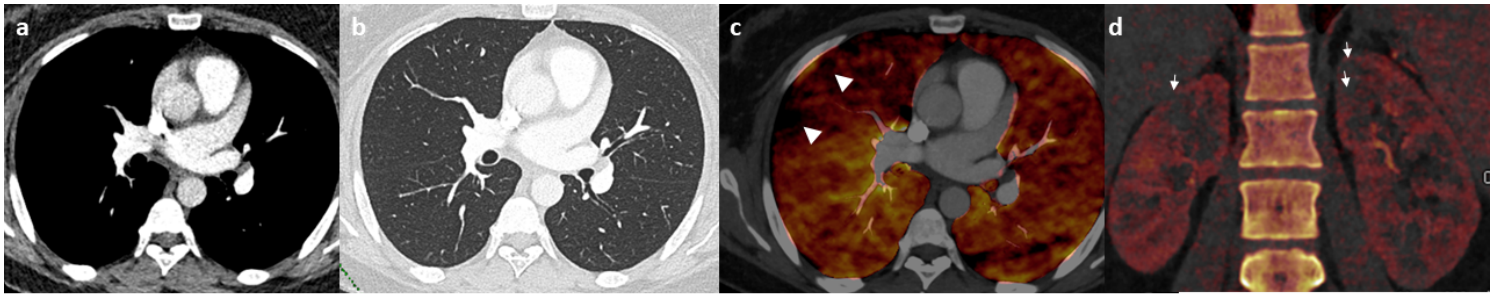

Figure 2

A 36-year-old female with coronavirus disease 2019 (COVID 19). No evidence of a PE can be seen on contrast-enhanced dual-energy computed tomography (DECT) angiography (a and b). On the perfusion

map images (c), perfusion deficits (arrowheads) can be seen in both lungs. On the coronal renal perfusion images (d), heterogeneous kidney enhancement with perfusion deficits (arrows) can be seen.

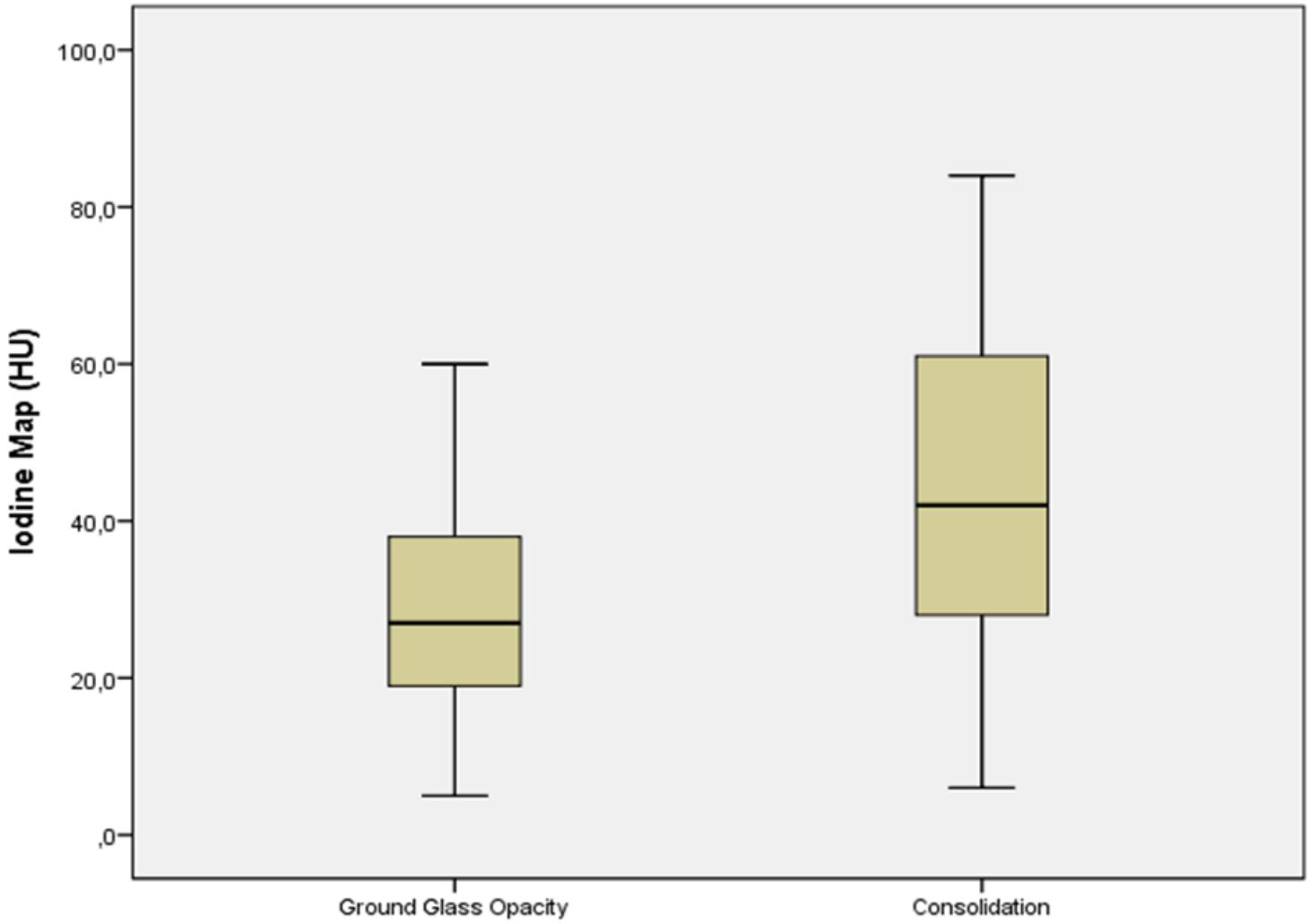

Figure 3

Boxplot shows the difference between iodine uptake of GGOs and consolidations.

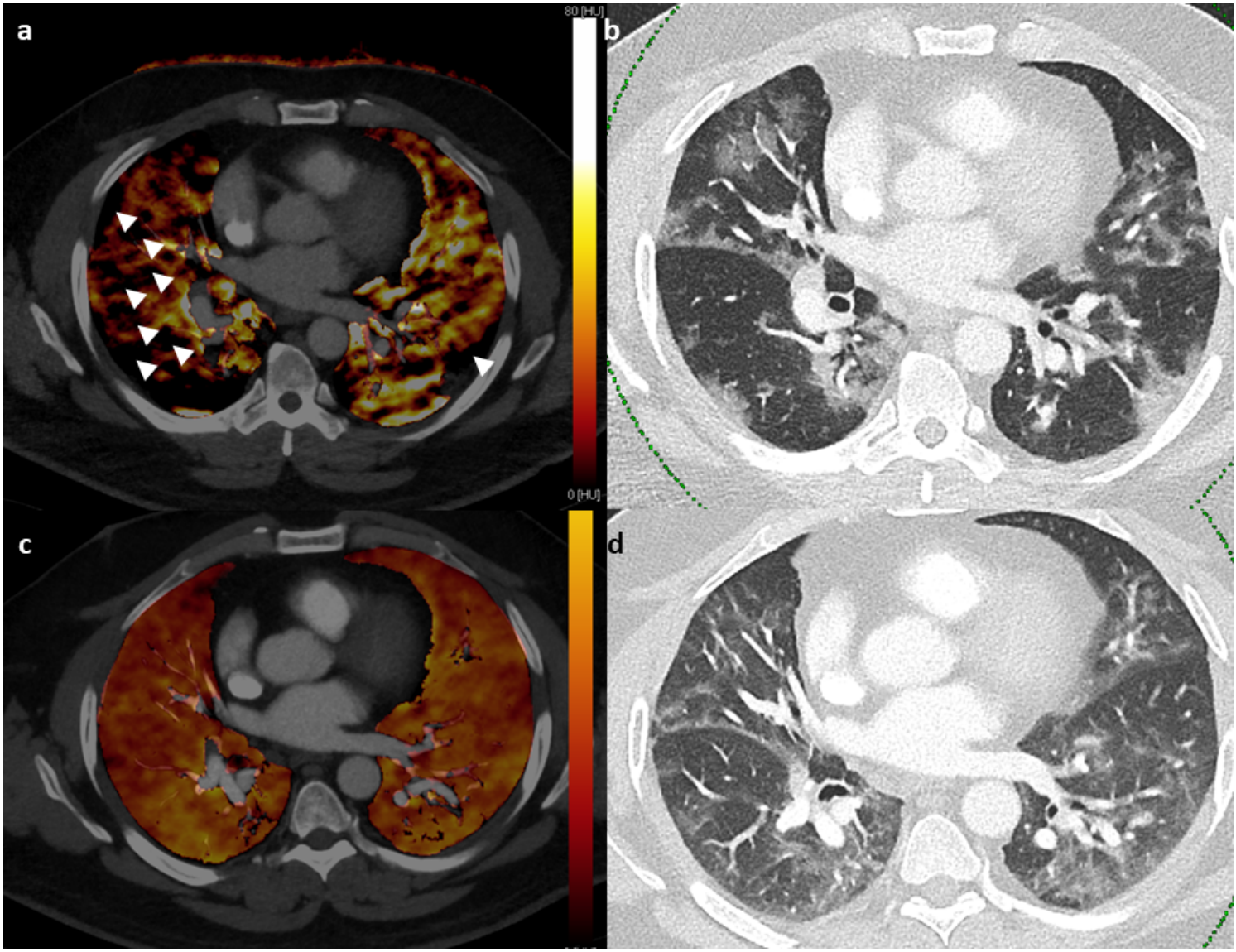

Figure 4

A 47-year-old male with coronavirus disease 2019 (COVID-19). The dual-energy computed tomography (DECT) angiography perfusion map (a) demonstrates multiple perfusion deficits, especially in the right lung (arrowheads). These areas do not match with the multiple ground-glass opacities seen on conventional CT (b). Follow-up DECT angiography 25 days after the first exam. Perfusion map (c) and conventional CT images (d) demonstrate more prominent regression in the perfusion deficits compared to the conventional CT findings.

Supplementary Files

This is a list of supplementary files associated with this preprint. Click to download.

- Supplementarytable1.docx
- Supplementarytable2.docx

- Supplementarytable3.docx
- Supplementarytable4.docx